

Molecular motions and ordering of the interfacial, droplet and binder regions of polymer dispersed liquid crystal displays: A paramagnetic resonance spin probe study

Y. C. Kim,^{a)} S. H. Lee, J. L. West, and E. Gelerinter^{b)}

Liquid Crystal Institute and Physics Department, Kent State University, Kent, Ohio 44242

Received 20 May 1994; accepted for publication 18 November 1994)

The molecular dynamics and ordering of polymer-dispersed liquid-crystal displays are studied using the technique of paramagnetic resonance of spin probes. A complex spectrum is observed in which components are identified from probes dissolved in the droplet, binder, and interfacial regions of the display. In particular, the liquid-crystal curing, phase separation, and structure of displays with both thermoplastic and epoxy binders are investigated. Observations are also performed as the liquid-crystal droplet size is varied. Among the more interesting results is the demonstrated ability to observe the interfacial region. It appears to be quite fluid and has little or no average order. It is also observed that the compatibility between the binder and liquid crystal, seen from some of the formulations studied, correlates with the reported electro-optical properties. These include the magnitude and hysteresis of switching voltages and the magnitudes of switching times. © 1995 American Institute of Physics.

I. INTRODUCTION

In this work we apply electron paramagnetic resonance (EPR) to the study of polymer-dispersed liquid-crystal (PDLC) displays. In particular, we investigate the phase separation and structure of PDLCs. EPR has been extensively used by us and others to study glass-forming materials.¹⁻¹² The materials studied include isotropic liquids, liquid crystals, polymers, and liquid-crystal polymers (LCPs). These studies yielded information concerning molecular dynamics and ordering over a considerable temperature range.

Research over the last decade has identified a wide variety of polymer/liquid-crystal composites that operate on the principle of electrically controlled light scattering.^{13,14} In particular, PDLCs consist of liquid-crystal droplets dispersed in a polymer binder and are formed by phase separation of a homogeneous solution of a liquid crystal and polymer. The orientation of the director in the liquid-crystal droplet is, in general, random from droplet to droplet, but the magnetic field of the EPR spectrometer is sufficient to align these directors. To a first approximation the PDLC materials can be viewed as combining the structural and film-forming characteristics of polymers with the electro-optic properties of low-molecular-weight liquid crystals; however, this is a crude approximation because the polymer, as well as the droplet size and shape, and the properties of the liquid crystal have a major influence on the electro-optic properties of these composites. These include the on- and off-state transmission, driving voltage, switching speed, hysteresis, and dielectric properties. For example the driving voltage of a PDLC film depends on the dielectric anisotropy, elastic constants, and

viscosity of the low-molecular-weight liquid crystal in addition to the film thickness and droplet size and shape. The polymer matrix also affects the electro-optics of PDLC materials. The dielectric properties of the polymer matrix can dramatically change the driving voltage of PDLC shutters by conductive shielding.^{15,16} Recent results have shown that the electro-optic properties of PDLC films change abruptly at the glass transition temperature T_g of the polymer matrix.^{17,18} This change in the electro-optic properties is most likely the result of changes in the surface anchoring energy at the polymer glass transition. The interface at the droplet wall of a PDLC is responsible for controlling this surface anchoring energy. Here we report the first study of the important interfacial region, the liquid-crystal droplet region, and the polymer matrix region using EPR. Spectral components originating from each of these three regions are observed. To help identify spectral features we observe spectra from probes dissolved in polymer-rich material and from probes dissolved in the liquid crystal. In the former case the observed spectra are quite similar to those we have assigned to the polymer binder. In the latter case the observed spectra are quite similar to those we have assigned to the liquid-crystal droplet. The spectra from the interfacial region should vary with droplet size. Smaller droplet size will increase the proportion of the interfacial region with a concomitant increase in the intensity in the spectral component assigned to the interfacial region. We demonstrate that this is exactly what is observed giving credence to our spectral assignments. We also demonstrate that EPR easily detects phase separation and the results correlate with the results detected using other techniques.

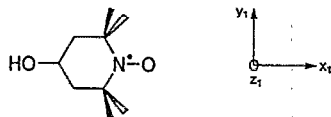
II. EXPERIMENT

The EPR nitroxide probes used in these studies are the small, nearly spherical (aspect ratio 1.2) tempol (TPL) molecule and the larger, cigar-shaped (aspect ratio 4.8) cholest-

^{a)} Author to whom all correspondence should be addressed.

^{b)} Permanent address: Polymer Materials Laboratory, Korea Institute of Science and Technology, P.O. Box 131, Cheongryang, Seoul, Korea.

Tempol (TPL)



Cholestane (COL)



FIG. 1. Spin probes used in this study.

tane (COL) molecule (see Fig. 1). Comparing the observed EPR spectra with those obtained from spectral simulations we are able to extract parameters such as molecular ordering, rotational relaxation times, and the temperature which is the boundary between slow and fast motion T_{50} .¹⁻¹² Some authors¹⁹⁻²¹ argue that T_{50} may be determined by interactions between the probe and the polymer.

Two of the samples studied are thermoplastic polymer-based PDLCs that are formed by thermally induced phase separation (TIPS).²² The first samples used polyvinyl formal (PVFM) from Aldrich Chemicals Co., Inc., as the matrix polymer and E63 from BDH, Ltd., as the dispersed liquid crystal. PVFM/E63 samples were made by mixing the components with 200 ppm by weight of the spin probe and a solvent (dichloromethane). The material was obtained as a film on a petri dish by drying the solution overnight at 90 °C in a mechanical convection oven. A 4:6 mixture of PVFM and E63 underwent phase separation as the solvent evaporated to form a PDLC film, but an 8:2 mixture remained homogeneous, mimicking the continuous polymer-rich binder. The second sample made by the TIPS method was a mixture of 40% of medium molecular weight polymethylmethacrylate (PMMA) and 60% E7 from BHD, Ltd. The droplet size for the TIPS samples was controlled by cooling rates. The PVFM/E63 was heated to 130 °C and quenched in a water bath to obtain small droplets. It was cooled at 1 °C/min to get larger droplets. The PMMA/E7 sample was treated in a similar manner after it was heated to 90 °C.

PDLCs prepared by the polymerization-induced phase separation (PIPS) method utilized a thermally cured epoxy formulated at the KSU Liquid Crystal Institute. The sample, epoxy/E7 (6:4), consisted of 9.1% EPON 828 (Shell Chemical), 33.8% of Capcure 3-800 (Miller-Stephens Chemical Co., Inc.), 17.1% of Heloxy 97 (Rhône-Poulenc), 40% E7, and 200 ppm by weight of a probe. 200 ppm of the probe in dichloromethane was added to E7 and the mixture was held at 70 °C overnight to remove the solvent. The liquid crystal and epoxy were then thoroughly mixed until the mixture appeared homogeneous and transparent. The time at which

TABLE I. Phase transition temperature of liquid crystals and polymers.

Materials	T_g (°C) ^a	T_{NI} (°C) ^a
E63	...	88 ^b
E7	...	61 ^b
PVFM	94	...
PVFM/E63 (8:2)	54	...
PVFM/E63 (4:6)	40	82-99
PMMA	105	...
PMMA/Eu (4:6)	42	50-67
Epoxy/E7 (6:4)		
Cured at 45 °C	23	45-73
Cured at 90 °C	28	46-70

^aTransition temperatures were measured by DSC at a scan rate of 10 °C/min.

^bE. Merck, Merck Industrial Chemicals, Poole, England.

the sample became transparent was taken as the start of the cure. It was then degassed in a centrifuge. The sample was placed in a 3-mm-i.d. sample tube and cured either in the EPR cavity or in a mechanical convection oven. Droplet size was controlled by the cure temperature. Curing temperatures varied from 90 to 45 °C with corresponding times for the onset of cure, as observed by light scattering and differential scanning calorimetry (DSC) experiments, from 2/3 to 4 h, respectively. Smaller droplets were obtained by curing the sample at 90 °C for 2 h, and larger droplets were obtained by curing the sample at 45 °C for 20 h. EPR indicated that the samples were stable for at least a few weeks.

A room-temperature PIPS sample was prepared using a commercial two-component 5 min epoxy (5MEP) that was cured at 25 °C. Here again E7 was used as the liquid crystal. Samples containing 40% and 50% liquid crystal [5MEP/E7 (6:4) and 5MEP/E7 (5:5)] were studied. Pure 5MEP and 5MEP plasticized with 10% E7 were used to check the position of the cholestane peaks in the cross-linked epoxy phase. Epoxy samples that did not contain liquid crystals were not degassed because they were very viscous and set quite fast. The properties of the materials used are summarized in Table I.

The EPR spectra were observed using an IBM X-band spectrometer with a variable-temperature controller accessory. Unless otherwise indicated, all spectra were taken at 25 °C. A spin-probe concentration of 200 ppm by weight gave a reasonable signal-to-noise ratio without dipolar broadening. The magnetic field was monitored by a Hall probe that had been previously calibrated near $g=2$ using a nuclear-magnetic-resonance magnetometer. The spectrometer frequency was measured using a Hewlett-Packard microwave frequency counter. Data were gathered and processed using an IBM CS9000 computer with EPR software supplied by the manufacturer.

Thermal properties of the PVFM/E63 mixtures and components were measured with a Perkin-Elmer DSC-7 calorimeter. Prior to heating scans the samples were held at 130 °C for 3 min and then cooled to -10 °C at a rate of 10 °C/min to erase any thermal history. DSC thermograms were obtained using a 10 °C/min scan rate from -10 °C. The phase behavior of the samples was observed using a Leitz Laborlux

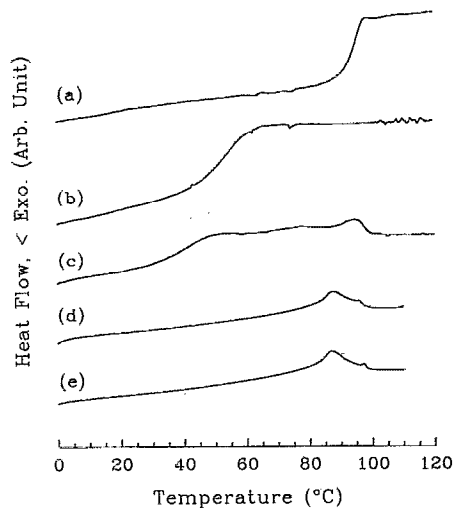


FIG. 2. DSC thermograms: (a) PVFM; (b) PVFM/E63 (8:2); (c) PVFM/E63 (4:6); (d) E63; (e) E63+200 ppm by weight of COL.

12 Pol polarizing microscope equipped with a Mettler FP 82 hot stage and a Mettler FP 80 central processor.

Scanning electron microscope (SEM) studies were performed using a Jeol JSM-6300V SEM.

III. RESULTS

A. DSC and optical microscopy

The DSC thermograms of the materials associated with PVFM/E63 sample are shown in Fig. 2. The T_g of the homogeneous 8:2 mixture (54 °C) is considerably higher than T_g of the 4:6 mixture (40 °C) implying that more liquid crystals can be dissolved in the polymer matrix without causing phase separation. The 8:2 material is a good approximation of the polymer-rich binder portion of the 4:6 PDLC so that the EPR spectra for 8:2 will help identify the part of the PDLC that is associated with the polymer-rich binder. It is also important to note that the addition of the col probe does little to change the thermal properties of the E63. T_{NI} for the liquid-crystal-rich phase of the 4:6 sample is observed to be higher than that of pure E63. Both the liquid-crystal-rich phase in the 4:6 mixture and the E63 displayed broad nematic-to-isotropic (NI) transitions which are verified by polarized optical microscopy. When E63 is heated at 1 °C/min one observes optically that isotropic domains begin to form at ~83 °C. These domains grow and coalesce until a homogeneous isotropic phase was formed at ~92 °C. The width of the NI transition can be attributed to the fact that E63 is a mixture of liquid crystals.

Phase mixing of the 4:6 mixture is observed at ~123 °C (heating 1 °C/min) and phase separation is observed at ~117 °C (cooling 1 °C/min) using an optical microscope without crossed polarizers. Such observations are quite unusual since the mixture of isotropic liquid crystals and thermoplastic polymer is transparent with only a small refractive index difference between the components. Previously, phase contrast microscopy was required for such observations.²³

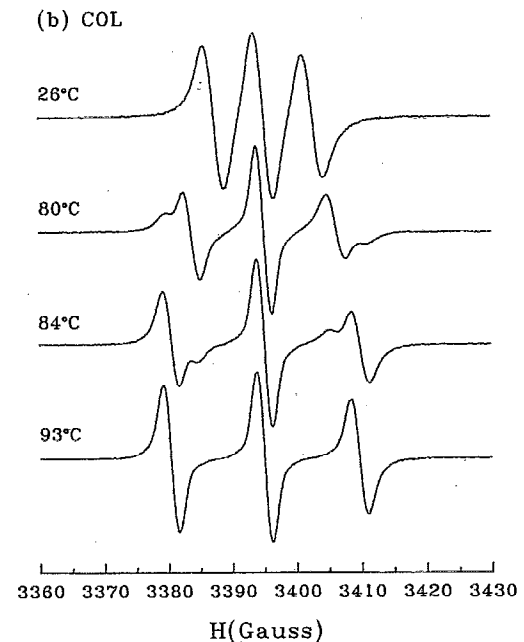
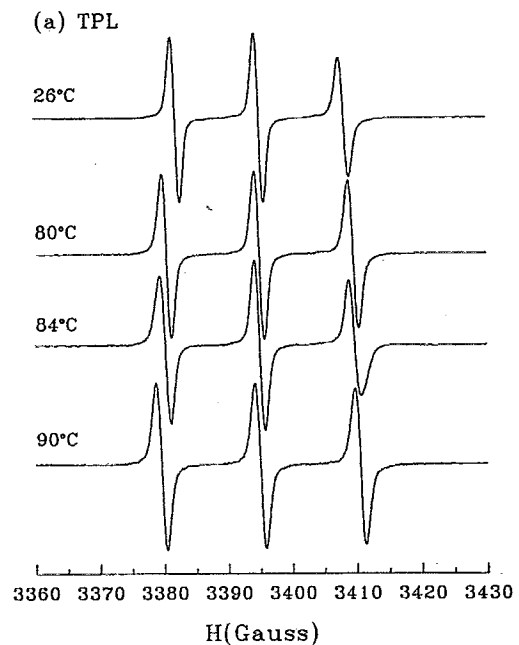


FIG. 3. EPR spectra from (a) TPL and (b) COL dissolved in E63 ($T_{NI}=88$ °C).

B. EPR and SEM results

Figure 3 displays the EPR spectra from TPL and COL dissolved in E63. Figure 4 plots the observed splittings versus temperature. The splittings in the nematic phase are smaller than those in the isotropic phase indicating the ordering of the probe by the liquid crystals. COL, being larger and having a larger aspect ratio, is ordered more than the TPL. The COL spectra taken at temperatures near the NI transition (88 °C) are seen to be composite spectra, i.e., one observes

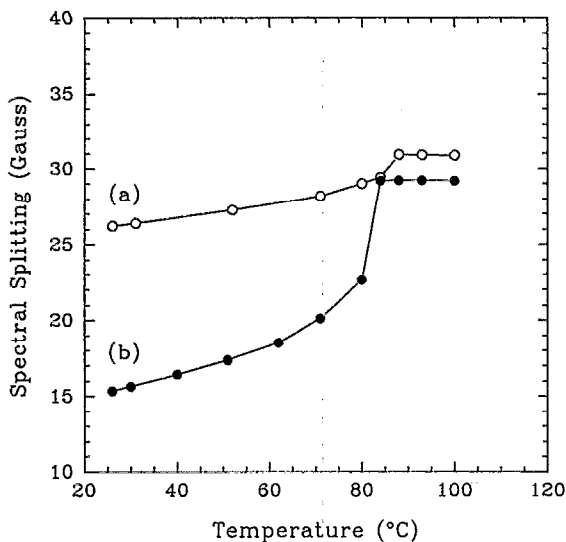


FIG. 4. Splitting vs temperature for (a) TPL and (b) COL dissolved in E63.

spectra from both the isotropic and nematic phases. These composite spectra are observed over a range of several degrees which is indicative of the broad transition previously observed in the DSC thermograms. The effect is not observed in the TPL spectra since the isotropic and nematic spectra near the NI transition are nearly the same. The EPR spectra consist of three well-resolved lines indicating that the probes are tumbling rapidly on the EPR time scale. The one exception to this is the 26 °C COL spectrum. Here no baseline exists between the individual broadened spectral lines indicating that the motions of the COL probe have started to slow down.

The situation is quite different when PVFM/E63 (8:2) is used as the solvent. The high-temperature spectrum from the TPL (~130 °C) indicates that the probe is moving reasonably quickly, and the low-temperature spectrum (~30 °C) indicates that the probe is standing still on the EPR time scale. The COL spectra indicate that the probe is moving slowly at high temperature and standing still on the EPR time scale at low temperature. This is very clearly indicated in Fig. 5 which is a plot of twice the Z component of the hyperfine splitting ($2A'_{zz}$) versus temperature. Here we can see the sharp boundary between slow and fast motion of the probe. Also note that T_{50} is 57 and 126 °C for TPL and COL, respectively, indicating the probe dependence discussed above.

When the TPL is dissolved in PVFM/E63 (4:6), one obtains the complex spectrum shown in Fig. 6. Three components are indicated. For reasons that will become clear as the discussion evolves, we associate 1 with the probe dissolved in the liquid-crystal droplet, 2 with the probe dissolved in the interfacial region, and 3 with the probe dissolved in the polymer-rich binder. The complex structure remains as the sample is heated until a temperature in the low 80s is reached. By the time the temperature reaches 85 °C, the structure is gone and one observes a three-line spectrum that is typical of nitroxide probes. The EPR data indicate that the

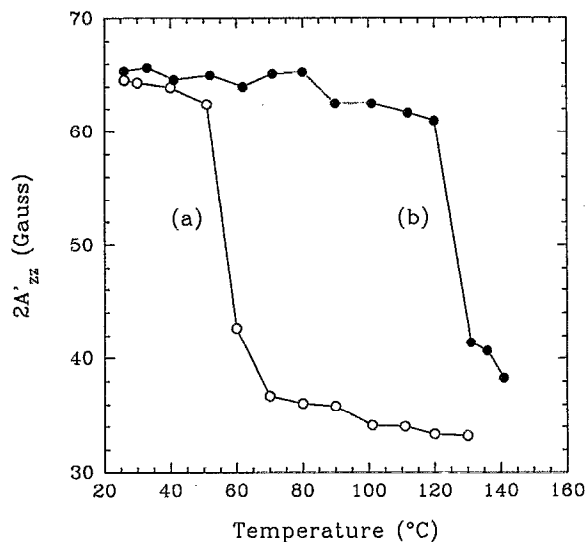


FIG. 5. Overall spectral width vs temperature for (a) TPL and (b) COL dissolved in PVFM/E63 (8:2).

sample has gone from a PDLC to a more homogeneous mixture of polymer and liquid crystal, but the optical microscopy observations indicate that phase mixing does not occur until 123 °C. Also, the liquid crystals are now partially in the isotropic phase ($T_{NI}=83-92$ °C). The spectrum from COL dissolved in PVFM/E63(4:6) is complex at intermediate temperatures but it becomes a simple three-line spectrum at ~100 °C. The DSC thermogram in Fig. 2 indicates that pure E63 displays a transition at approximately 90 °C which is between the values indicated by the TPL and COL data. As the temperature is reduced the spectral components broaden and become more difficult to resolve. This occurs because

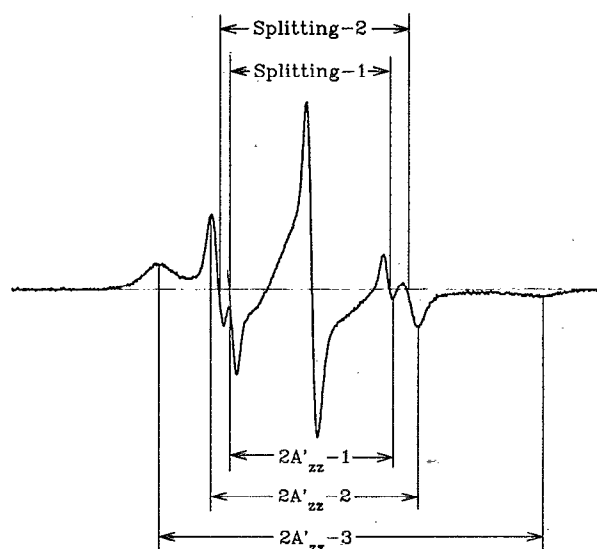


FIG. 6. EPR spectrum from TPL dissolved in PVFM/E63 (4:6) at 23 °C. The splittings and $2A'_{zz}$ values for components 1, 2, and 3 are indicated.

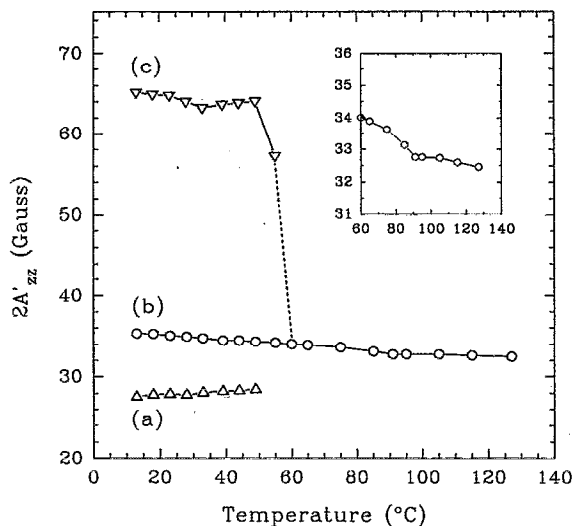


FIG. 7. Overall spectral width for TPL dissolved in PVFM/E63 (4:6): (a) component 1; (b) component 2; (c) component 3.

the larger COL probe is slowing down. One needs to be cautious when analyzing the data from the complex spectra. Measuring the splitting is difficult because of overlap of the components. In most cases measuring $2A'_{ZZ}$ is more straightforward since the peaks are easier to locate, but the apparent peak location can be slightly different than the real location due to the poor resolution of the spectral components. Nevertheless some definite trends can be observed.

In Fig. 7 we display a plot of $2A'_{ZZ}$ for TPL versus temperature for the three components. Component 1, which we associate with the liquid-crystal-rich droplet, displays values close to those of the neat E63 and the ordering appears to be slightly less. Presumably the latter is due to some polymer being present in the droplet. There is also the competing effect of surface ordering which is not present in the bulk liquid crystals. The director orientation is distorted by the curved morphology of the droplet. Component 3, which we associate with the polymer-rich binder displays a result quite similar to that obtained from PVFM/E63 (8:2). T_{50} is $\approx 55^\circ\text{C}$ in good agreement with the PVFM/E63 (8:2) data.

The data from component 2 are by far the most exciting since we associate them with the interfacial region. The data indicate that the probe in this region is not ordered, and the spectra indicate that the region is quite fluid. The increase in $2A'_{ZZ}$ as the temperature is reduced indicates that the probe is slowing down. It is interesting to note that the slope of the line changes abruptly at $\approx 95^\circ\text{C}$, which is just above the temperature at which the liquid crystals are completely isotropic.

Most of these conclusions are reinforced when one observes the corresponding COL data in Fig. 8. There is trouble gathering data for component 1 because of its proximity to the strong central line. The data from component 3 are quite similar to that observed for PVFM/E63 (8:2), but the observed $T_{50} \approx 90^\circ\text{C}$. This is larger than the value obtained for the TPL but less than that displayed by COL in PVFM/E63

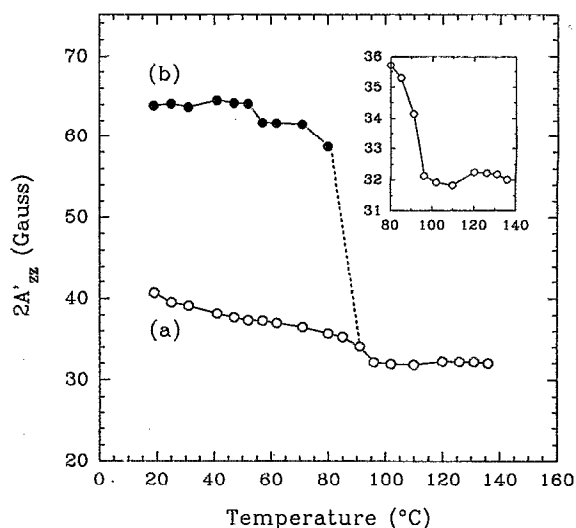


FIG. 8. Overall spectral width for COL dissolved in PVFM/E63 (4:6): (a) component 2; (b) component 3.

(8:2). The cholestane data from region 2 is qualitatively similar to that from the TPL. One observes the increase in $2A'_{ZZ}$ as the temperature is decreased and the change of slope at the phase separation temperature. Since cholestane is a much larger probe the effects described are larger. $2A'_{ZZ}$ goes to 40 G at 20°C compared with 35 G for the TPL. The COL data also indicate that the interfacial region is quite fluid and the probe's motion is isotropic.

The volume of the interfacial region can be varied by varying the liquid-crystal-rich droplet size. In Fig. 9 we show spectra from the TPL in PVFM/E63 (4:6) samples that have large (slowly cooled) and small (quickly cooled) droplets. SEM studies indicate that the droplets in slowly cooled samples have an average diameter of $7\ \mu\text{m}$ and those in the quickly cooled samples have an average diameter of $0.3\ \mu\text{m}$.

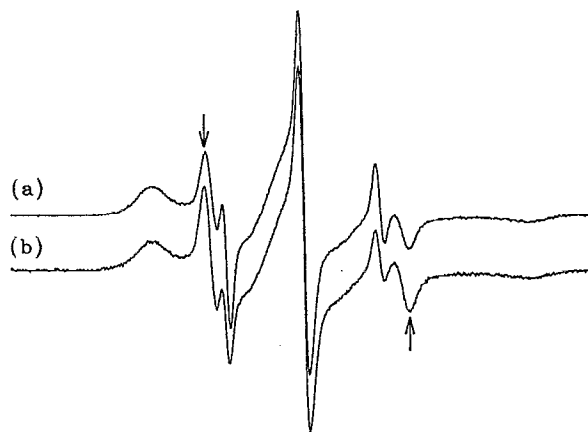


FIG. 9. Spectra illustrating the effect of liquid-crystal-rich droplet size upon the interfacial component for TPL (indicated by arrows) in PVFM/E63 (4:6): (a) larger droplets; (b) smaller droplets.

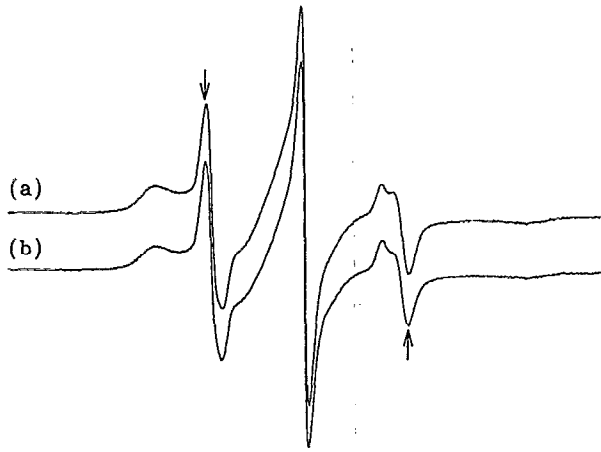


FIG. 10. Spectra illustrating the effect of liquid-crystal-rich droplet size upon the interfacial component for TPL (indicated by arrows) in PMMA/E7 (4:6): (a) larger droplets; (b) smaller droplets.

The amplitude of the spectrum from the interfacial region (marked by arrows) clearly grows while the droplet spectrum shrinks as the droplet size is reduced. The droplets appear to be ellipsoidal rather than spherical. The ellipsoidal droplets may result from the different thermal-expansion coefficients of the polymer and glass substrates.

A similar experiment was performed for the TPL in PMMA/E7 (4:6) and the results are shown in Fig. 10. The spectra from the liquid-crystal-rich droplet and the interfacial region are not as well resolved as for the previously described case. The boundary of the droplet may not be as well defined, or the droplet may contain more polymer than the droplet in the PVFM/E63 case. This would indicate that E7 and PMMA are more compatible than the PVFM/E63 combination. There is very little difference between the spectra from the slowly and quickly cooled samples which is consistent with the reduced liquid-crystal order in the droplet due to the presence of extra polymer. Our SEM studies for this case indicate an average droplet diameter of 4 μm for the slowly cooled case, and an average droplet diameter of 0.3 μm for the quickly cooled case. This ratio is slightly more than a half of that for the PVFM/E63 (4:6) case. The droplets are observed to be more spherical. These SEM observations also indicate greater compatibility of E7 and PMMA.

The results from epoxy/E7 (6:4) are the most dramatic. Spectra from samples cured at seven different temperatures were observed (90, 80, 70, 60, 55, 50, and 45 $^{\circ}\text{C}$ with corresponding cure times of 2, 3, 5, 8, 12, 16, and 20 h). SEM studies of these samples were also performed. Photographs of samples slowly cured at 45 $^{\circ}\text{C}$ displayed a bimodal distribution of droplet sizes. The larger droplets averaged 90 μm in diameter (much larger than the thermoplastic cases), and the smaller droplets averaged 4 μm in diameter. Most of the liquid crystals are in the larger droplets. For the case of samples quickly cured at 90 $^{\circ}\text{C}$, the average droplet diameter was 0.7 μm . This large difference in droplet size made for impressive EPR effects. As the curing temperature is raised

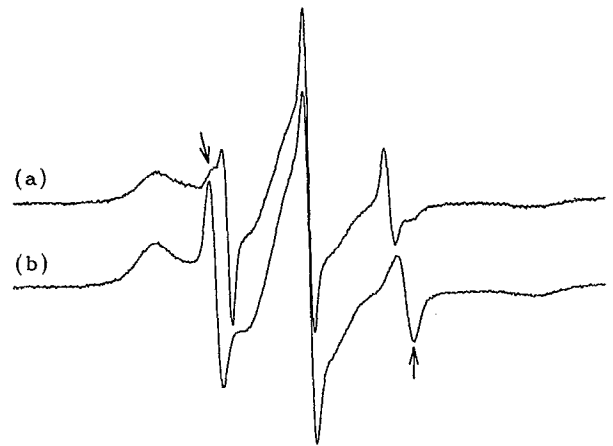


FIG. 11. Spectra illustrating the effect of liquid-crystal-rich droplet size upon the interfacial component for TPL (indicated by arrows) in epoxy/E7 (6:4): (a) larger droplets; (b) smaller droplets.

the droplet size is reduced, and we see dramatic growth of the signal from the interfacial region and dramatic reduction in the signal from the droplet. This is seen in Fig. 11 where spectra for the two extreme cases (90 and 45 $^{\circ}\text{C}$ cures) are shown.

The EPR technique can also be used to detect phase separations during curing. In Figs. 12(A) and 12(B) we display spectra from both probes in epoxy/E7 (6:4) before, during, and after curing at 45 $^{\circ}\text{C}$. Light scattering experiments indicate phase separation begins at approximately 240 min. In the COL [Fig. 12(B)] spectrum one sees the beginning of a droplet signal as indicated by an arrow at this time. This signal becomes much more obvious after the sample has been cooled to room temperature. The cholestane signal from the cured sample does not display the viscous signal that we associated with epoxy binder. The situation is a little different for the TPL probe [Fig. 12(A)]. Early in the cure we see one spectrum indicating fairly fast motion. Starting at 240 min both the viscous spectrum associated with the binder and the isotropic fluid spectrum appear and proceed to grow. When the cured sample is cooled to RT the three features associated with the PDLC appear, namely spectra from the binder, the interfacial region, and the liquid-crystal-rich droplet.

In Figs. 13(A) and 13(B) we show the results of a similar experiment using a 5MEP. The addition of liquid crystals raised the setting time for 5MEP/E7 (6:4) to approximately 15 min. The TPL [Fig. 13(A)] spectra shown have the same general features as the epoxy/E7 (6:4) data discussed above. The binder spectrum grows at the expense of the more fluid spectrum. The TPL does not appear to be ordered very much in the liquid-crystal-rich droplet making its signal hard to distinguish from the interfacial region's signal. Early in the cure the cholestane signal [Fig. 13(B)] indicates a highly viscous region. As the cure proceeds a signal indicating intermediate viscosity grows at the expense of the viscous signal. After 2 h have passed the viscous signal usually associ-

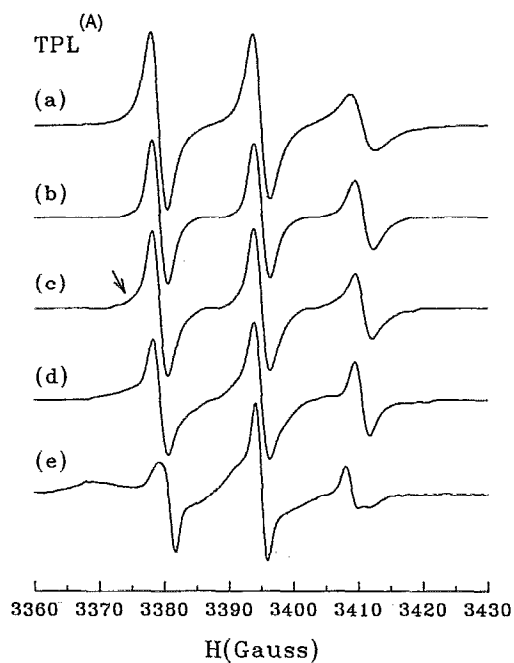


FIG. 12. Spectra from (A) TPL and (B) COL to illustrate curing in epoxy/E7 (6:4); approximately 4 h are required to cure at 45 °C: (a) observed at RT before cure; (b) observed at 45 °C 180 min into the cure; (c) observed at 45 °C 240 min into the cure; (d) observed at 45 °C 300 min into the cure; (e) observed at RT after the cure.

ated with the binder has disappeared and the intermediate signal, associated with the interfacial region, is quite strong. There is a hint of the signal associated with the droplets. Here, as in the case of epoxy/E7 (6:4) the signal from the binder appears to be missing. SEM photographs indicate a very small droplet size (0.5 μm) which accounts for the lack of signal from the droplets.

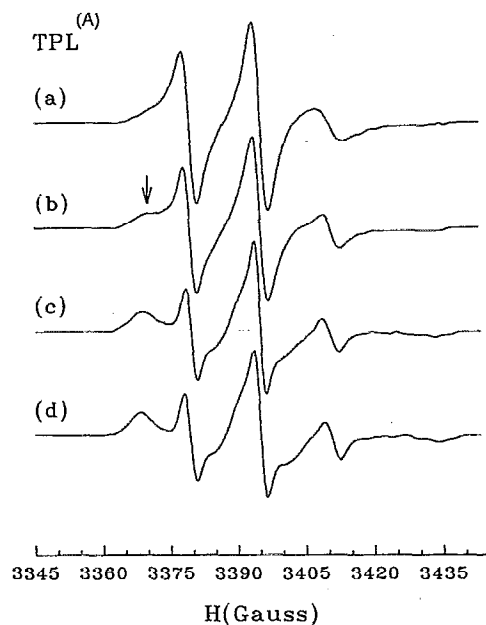


FIG. 13. Spectra from (A) TPL and (B) COL to illustrate curing in 5MEP/E7 (6:4); approximately 15 min are required to cure at 25 °C: (a) 14 min into the cure; (b) 20 min into the cure; (c) 40 min into the cure; (d) 90 min into the cure.

Spectra obtained from 5MEP/E7 (5:5) were similar to those obtained from 5MEP/E7 (6:4), but the signals from liquid-crystal-rich regions are more intense. SEM photographs indicate “droplets” of epoxy (3.8 μm) dispersed in liquid crystals. This structure occurs because of the higher concentration of liquid crystals and is also consistent with the larger liquid-crystal signal. The question of the disappearance of the COL binder signal as the PIPS process proceeded needs to be addressed. Two possible explanations

come to mind. One possibility is that the COL becomes less soluble in the epoxy as it cures so that it is expelled to the liquid-crystal-rich region. A second explanation is that COL reacts with the epoxy as it cures. To check this samples of COL in 5MEP/E7 (9:1) and 5MEP/E7 (10:0) (i.e., no liquid crystals) were studied. EPR spectra taken 3 days later, after the COL had time to react, displayed strong glassy signals indicating that little or no chemical reaction has taken place.

IV. DISCUSSION

The results of the EPR study provide new insights into the PDLC systems studied. The probes have clearly identified three regions in a PDLC: the liquid-crystal droplet, the polymer binder, and the interface. Each region is characterized by the mobility and order of the probe with the liquid-crystal droplet having the greatest mobility and order and the polymer binder having the least mobility and order. The phase separation process is monitored by observing the appearance of peaks associated with each region.

The interface region is isotropic or at least of very low order. This result is supported by recent studies using polarized ultraviolet absorption of thin liquid-crystal films coated on polymer alignment layers that show a low liquid-crystal order parameter near the polymer interface.²⁴ The low order of the interface may be the result of a relatively high polymer concentration in this region or it may be the result of the liquid crystals near the droplet wall being disordered by the polymer surface.

While the EPR spectra detect no order in the interfacial region, other considerations support at least minimal liquid-crystal order at the interface. EPR measures the average order of this region so that its detection of no order does not preclude minimal order at surface. If the interface were completely isotropic the liquid crystal droplet region would take on a radial configuration similar to the droplets that form during the isotropic to nematic phase transition where the nematic liquid-crystal droplets float in the isotropic fluid. The droplet director in the PVFM and PMMA binders is bipolar indicating at least a minimal order in the interface region. Also, if the interface did not impose a preferred orientation on the droplet director only thermal fluctuations would return the droplet directors to a random orientation upon removal of an aligning electric or magnetic field, resulting in a slow switching speed. However, PDLC films, and in particular PDLC films with a PVFM or PMMA binder, return rapidly to a random orientation upon removal of an aligning field. Therefore, the interface likely retains some residual order that controls the droplet configuration and director orientation.

The EPR probes also monitor changes in the physical properties of the regions with changes in temperature. Of particular interest is the relationship between the EPR spectral response of the TPL and COL probes and the electro-optic response of the PDLC materials. As outlined in the introduction, the EPR spectral response depends on the physical properties of the medium and the aspect ratio and size of the probe. This dependence is clearly seen in Fig. 5. The change in the motion of the polymer binder with tem-

perature is detected by each probe. Because of the much smaller size of the TPL probe the T_{50} occurs about 70 °C lower than the COL probe. The T_{50} for the TPL probe occurs close to the T_g of the polymer binder as measured by DSC and temperature where electro-optic properties of the PDLC change abruptly.

The EPR results also shed light on the causes of the abrupt change in electro-optic properties of the PVFM/E63 PDLC at the binder T_g . At the binder T_g the switching voltage rapidly decreases, and the switching time and hysteresis increase. Figure 7 shows a dramatic change in the EPR spectra of the same PVFM/E63 system at about the same temperature. At lower temperatures the spectra from the droplet, interface, and polymer binder are clearly delineated whereas at higher temperatures only a single spectral component is resolved. The merging of the spectral components at higher temperatures results from an increase in the compatibility of the liquid crystals and the polymer. The increased compatibility may have several effects on the electro-optic response. The increased compatibility may lower the anchoring energy of the liquid crystals at the droplet wall which would reduce the driving voltage and increase the switching time. Also the increased compatibility may result in a more fluid interface that would realign with the liquid crystals. This realignment of the interface would result in the observed increase in the hysteresis of the electro-optic response. The EPR spectra of the epoxy and PMMA binder PDLCs also show greater compatibility of the liquid crystals and polymer and these systems have lower driving voltages, higher switching times, and larger hysteresis than the PVFM/E63 system below the binder T_g .

EPR is a useful tool for characterization of the formation and physical properties of PDLC materials. In particular, the EPR spectra have clearly identified and characterized the interface between the liquid crystals and polymer binder and related changes in the compatibility of the liquid crystals and polymer to the electro-optic response of the PDLC shutters.

ACKNOWLEDGMENT

Research was supported in part by the NSF Science and Technology Center ALCOM, DMR 89-20147.

- 1 J. I. Spielberg and E. Gelerinter, *Phys. Rev. A* **32**, 3647 (1985).
- 2 J. I. Spielberg and E. Gelerinter, *Phys. Rev. B* **30**, 2319 (1984).
- 3 J. I. Spielberg and E. Gelerinter, *J. Chem. Phys.* **77**, 2159 (1982).
- 4 J. I. Spielberg and E. Gelerinter, *Chem. Phys. Lett.* **92**, 184 (1982).
- 5 J. F. Morris and E. Gelerinter, *Polymer* **30**, 165 (1989).
- 6 J. Li and E. Gelerinter, *Polymer* **33**, 963 (1992).
- 7 P. Krishnan, H. Le, S. H. Lee, and E. Gelerinter, *J. Polymer Sci. B* **31**, 1885 (1993).
- 8 A. T. Bullock, G. G. Cameron, and I. S. Miles, *Polymer* **23**, 1536 (1982).
- 9 I. S. Miles, G. G. Cameron, and A. T. Bullock, *Polymer* **27**, 190 (1986).
- 10 P. Törmälä, *J. Macromol. Sci. Rev. Macromol. Chem. C* **17**, 297 (1979).
- 11 S. H. Lee and E. Gelerinter, *Polymer* **35**, 2725 (1994).
- 12 S. H. Lee, V. Surendranath, Y. C. Kim, and E. Gelerinter, *Liq. Cryst.* (to be published).
- 13 J. L. West, in *Liquid Crystal Polymers*, edited by R. A. Weiss and C. K. Ober, ACS Symposium Series 435 (ACS, Washington, DC, 1990), p. 475.
- 14 J. W. Doane, in *Liquid Crystals, Applications and Uses*, edited by B.

- Bahadur (World Scientific, London, 1990), Vol. 1, p. 362.
- ¹⁵J. R. Kelly and D. Seekola, Proc. SPIE **17**, 1257 (1990).
- ¹⁶D. Seekola and J. R. Kelly, Proc. SPIE **19**, 1455 (1991).
- ¹⁷J. L. West, J. R. Kelly, K. Jewell, and Y. Ji, Appl. Phys. Lett. **60**, 3238 (1992).
- ¹⁸Y. Ji, J. R. Kelly, and J. L. West, Liq. Cryst. **14**, 1885 (1993).
- ¹⁹G. P. Rabold, J. Poly Sci. A-1, 1203 (1969).
- ²⁰P. L. Kumler and R. F. Boyer, Macromolecules **9**, 903 (1976).
- ²¹N. Kusumoto, S. Sano, N. Naitsu, and Y. Motozato, Polymer **17**, 448 (1976).
- ²²J. L. West, Mol. Cryst. Liq. Cryst. Inc. Nonlin. Opt. **157**, 427 (1988).
- ²³W. Ahn, C. Y. Kim, H. Kim, and S. C. Kim, Macromolecules **25**, 5002 (1992).
- ²⁴J. L. West, S. Kobayashi, and Y. Imura (unpublished).